

Hopf bifurcation in a flux qubit coupled to a nanomechanical oscillator

Lior Ella* and Eyal Buks

Department of Electrical Engineering, Technion, Haifa 32000 Israel

(Dated: March 10, 2019)

We study the nonlinear semiclassical dynamics of a driven flux qubit coupled to a nanomechanical oscillator. While both of these systems are dissipative, their mutual coupling can effectively suppress the dissipation, and can lead to a loss of stability and to an emergence of synchronized self-excited oscillations of the system as a whole, at a time scale set by the mechanical beam. In this article we argue this by obtaining a set of semiclassical, nonlinear equations of motion for the two coupled subsystems, and showing that this system undergoes a supercritical Hopf bifurcation as the coupling is increased. We derive analytical expressions for the critical coupling coefficient and the renormalized mechanical dissipation coefficient and frequency, and give a complete characterization of the limit cycle behavior when the qubit and the oscillator are near resonance.

PACS numbers: 85.85.+j, 85.25.Dq, 05.45.-a

I. INTRODUCTION

The nano-electromechanical system comprised of a driven flux qubit coupled to an oscillating beam has recently become the subject of a great deal of research^{1–17}, due to its potential for the preparation of macroscopic non-classical states of the nanomechanical beam^{1–7} and for the realization of high-precision position detectors^{8,17}. Since the coupling between the qubit and oscillator is nonlinear, the semiclassical dynamics of the system may exhibit a wide range of typical nonlinear behavior, such as loss of stability and limit cycle oscillations. A characterization of these dynamics is therefore important for an experimental realization of these systems, and may also hint at possible directions for the preparation of non-classical states of the mechanical oscillator.

In this article we provide a detailed characterization of the weakly nonlinear behavior in this system. In particular, we show that when the coupling between the qubit and the oscillator, which is assumed to be small, is increased beyond a certain threshold, the system begins to exhibit limit cycle behavior, with the qubit and the beam undergoing synchronized oscillations at the renormalized oscillation frequency of the beam. While the stability properties of this system, and of the analogous system of a flux qubit coupled to an LC resonator, have been investigated in Refs. 5, 18–24, our approach is unique by the fact that we provide a detailed characterization of the dynamical behavior of the system beyond its stability threshold, using analytical tools from the theory of nonlinear dynamical systems. Using these methods, we derive analytical expressions for the critical coupling coefficients, the renormalized mechanical dissipation coefficient, the amplitude and the frequency of the self-excited oscillations, in terms of directly measurable experimental quantities. We supplement these analytical expressions with numerical analysis and simulation.

The system we investigate consists of a flux-driven rf superconducting quantum interference device (SQUID), integrated with a mechanical resonator in the shape of a doubly clamped beam. As shown in Refs. 25–30, this

type of system can function as a qubit, exhibiting coherent quantum dynamics. The motion of the mechanical resonator can be approximated as that of a single-mode harmonic oscillator. This oscillator affects the dynamics of the qubit by varying the amount of flux threading the loop of the SQUID, which alters its energy level splitting. The qubit, in turn, affects the dynamics of the oscillator by applying a transverse Lorentz force, which is proportional to the current in the loop and the magnetic field at the location of the beam. In this article, we consider a single Josephson junction (JJ) rf SQUID due to its simplicity. In practice, however, the flux qubit is implemented using an asymmetric configuration of three or four Josephson junctions known as a persistent current qubit^{28,29,31}, owing to its superior noise characteristics.

It has been shown^{5,18,20} both theoretically and experimentally that the coupling between the oscillator and the qubit can lead to a renormalization of the oscillator's dissipation coefficient through a process known as “Sisyphus amplification and cooling”: When the driving frequency of the qubit (or one of its harmonics) is larger than the energy level separation, the system is said to be blue-detuned, and the excess energy in each photon is partially transferred to the oscillator, effectively lowering its dissipation coefficient. When the driving frequency is smaller than the energy level separation, the system is said to be red-detuned, and the opposite occurs³².

Consider the case of a blue-detuned system. When the coupling, which is controlled by the applied magnetic field at the location of the beam, is strong enough, the effective mechanical dissipation coefficient can become negative. When this occurs, the system will undergo a Hopf bifurcation and exhibit self-excited oscillations. In this article we provide a characterization of these oscillations, and qualitatively discuss their consequences for the generation of non-classical states of the oscillator.

The article is organized as follows. In section II we derive the semiclassical dynamical equations from first principles. This section follows closely the work in Refs. 2 and 7. In section III we perform an analysis of these dynamical equations. In subsection III B we determine the

stability properties of the linearized system, which are identical to those of the full system. In subsection III C we derive a complete analytical characterization of the limit-cycle behavior of the system when the oscillator and the qubit are resonant, which includes expressions for the amplitude, frequency and phase of the limit cycle. Finally, in section IV, we discuss the possible uses of these results and outline directions for future progress.

II. DERIVATION OF DYNAMICAL SYSTEM

In this section we derive a set of evolution equations for the averages of the operators of the qubit and oscillator, under the assumption that these averages factorize. We begin with the Hamiltonian of the rf SQUID and the mechanical oscillator, from which we derive an effective two-level Hamiltonian for the two lowest-lying persistent current states of the SQUID. We then include the effects of the environment by incorporating three reservoirs, which account for the relaxation of the oscillator and for the relaxation and dephasing of the qubit. These lead to Bloch-Langevin type equations for the qubit and a Langevin equation for the oscillator, from which we derive the dynamical system under investigation. This is found by taking the averages of the equations, and assuming that the reservoirs are in thermal equilibrium, and that the correlations between the qubit and the oscillator are sufficiently small to be neglected in the evolution equations.

A. Description of the system

In this section we recapitulate the main results given in Refs. 2 and 7. The system consists of an rf SQUID with a single Josephson junction integrated with a doubly clamped beam which is free to oscillate⁶, as shown in Fig. 1. The loop of the SQUID is threaded by a magnetic flux given by

$$\Phi_t = \Phi_e + LI_L + BlX, \quad (1)$$

where Φ_e is an externally applied flux, L is the inductance of the loop, B is the magnetic field at the location of the loop, X is the displacement of the beam and l is its effective length.

1. Hamiltonian

The combined system of the qubit and oscillator is described by the Hamiltonian

$$H_0 = \frac{P^2}{2m} + \frac{Q^2}{2C} + U, \quad (2)$$

with

$$U(\Phi_t, X) = \frac{1}{2}m\omega_m^2 X^2 + \frac{1}{2L}(\Phi_t - \Phi_e - BlX)^2 + E_J \left(1 - \cos \left(\frac{2\pi\Phi_t}{\Phi_0} \right) \right). \quad (3)$$

Here m is the mass of the beam, C is the capacitance of the Josephson junction, ω_m is the natural frequency of the beam, and $E_J = \Phi_0 I_c / 2\pi$, with $\Phi_0 = \hbar/2e$ and I_c is the critical current of the junction. P and Q are the momentum of the beam and the charge of the junction capacitance, respectively, and we have $[X, P] = [\Phi_t, Q] = i\hbar$.

2. Normalized coordinates

Introducing normalized coordinates

$$\begin{aligned} \phi_t &= \frac{2\pi\Phi_t}{\Phi_0} + \pi \\ q &= \frac{2\pi Bl}{\Phi_0} X \\ \phi_e &= \frac{2\pi\Phi_e}{\Phi_0} + \pi, \end{aligned} \quad (4)$$

we write the potential (3) as

$$\begin{aligned} U(\phi_t, q) &= E_J \left(\cos \phi_t - 1 + \frac{1}{2\beta_L} (\phi_t - \phi_e - q)^2 \right) \\ &+ \frac{1}{2}m \left(\frac{\omega_m \Phi_0}{2\pi Bl} \right)^2 q^2, \end{aligned} \quad (5)$$

where $\beta_L = 2\pi LI_c / \Phi_0$. In addition, we define a current operator

$$I = -\frac{2\pi}{\Phi_0} \frac{\partial H}{\partial \phi_e}. \quad (6)$$

This operator corresponds to the persistent current circling the loop. Assuming also that $\beta_L \gtrsim 1$, the potential, as a function of ϕ_t , has two shallow wells. Each of these wells gives rise to a localized phase state, or equivalently, to a localized current state. Since the separation of the wells is of the order of unity, and I_c is of a macroscopic size, these two states correspond to macroscopically distinguishable currents, which we label $|\odot\rangle$ and $|\oslash\rangle$. Furthermore, the external flux driving is assumed to have both DC and AC components, and is given by

$$\phi_e = \phi_{e0} + \phi_{e1} \cos \omega_d t.$$

B. Effective Hamiltonian of the qubit and oscillator

When $\langle \phi_t \rangle \gg \phi_e, q$ and $\beta_L \gtrsim 1$, the two lowest-lying energy levels, whose eigenstates are linear combinations

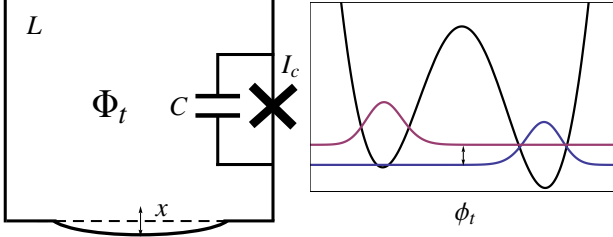


FIG. 1. (Color online) The qubit-oscillator system, as described in II A. The inset shows the potential (3) as a function of ϕ_t for a certain value of $\phi_e + q$, and both of the localized flux wavefunctions with lowest energies. The wavefunction on the left-hand side corresponds to the state $|\Downarrow\rangle$, and the wavefunction on the right-hand side to $|\Uparrow\rangle$. The time variation of $\phi_e + q$ in (3) gives rise to transitions between these two states.

of $|\Downarrow\rangle$ and $|\Uparrow\rangle$, are far from the energy levels above. When, in addition, the temperature is sufficiently low, it can be assumed that these are the only occupied levels. In this case, the SQUID can be approximated as a qubit, as described in Ref. 2. The circulating current can be found using (6): its eigenvalues are $\pm I_{cc}$, where

$$I_{cc} = I_c \frac{\phi_{t,\min}}{\beta_L},$$

and $\phi_{t,\min}$ is the normalized flux at the minima of the potential, which can be found approximately by expanding (5) to obtain a quadratic polynomial, giving

$$\phi_{t,\min} = \sqrt{6 \left(1 - \frac{1}{\beta_L}\right)}. \quad (7)$$

The Hamiltonian of the qubit and the oscillator is then given by

$$H_S = \frac{\varepsilon_0}{2} (\phi_{e0} + \phi_{e1} \cos \omega_d t) \sigma_z + \frac{1}{2} \hbar \Delta \sigma_x + \hbar \omega_m \left(a^\dagger a + \frac{1}{2} \right) + \frac{1}{2} \hbar k (a + a^\dagger) \sigma_z, \quad (8)$$

where σ_x and σ_z are the Pauli matrices,

$$\varepsilon_0 \simeq \frac{2E_J}{\beta_L} \sqrt{6 \left(1 - \frac{1}{\beta_L}\right)}, \quad (9)$$

$$\Delta \simeq \frac{3}{2} E_J \left(1 - \frac{1}{\beta_L}\right)^2,$$

and $\hbar k = B I_{cc} \sqrt{\frac{\hbar}{2m\omega_m}}$ is the coupling energy between the qubit and the oscillator.

C. Coupling to the environment

1. Model of the environment

The relaxation properties of the qubit and oscillator play a pivotal role in the dynamics of this system, and, indeed, are the focus of this article. Therefore any valid description must include the effects of coupling to the environment. We will model the main sources of relaxation as bosonic reservoirs coupled linearly to the qubit and oscillator, and consider three types of relaxation processes: thermal relaxation of both the qubit and oscillator, and dephasing due to fluctuations in the magnetic field threading the loop. The Hamiltonian accounting for these reservoirs is

$$H_R = \int d\omega \hbar \omega c_m^\dagger(\omega) c_m(\omega) + \int d\omega \hbar \omega c_{q1}^\dagger(\omega) c_{q1}(\omega) + \int d\omega \hbar \omega c_{q\varphi}^\dagger(\omega) c_{q\varphi}(\omega), \quad (10)$$

where the boson operators $c_i(\omega)$ and $c_i^\dagger(\omega)$, with $i = m, q_1, q_\varphi$, satisfy the usual commutation relations

$$[c_i(\omega), c_j^\dagger(\omega')] = \delta_{ij} \delta(\omega - \omega'),$$

where δ_{ij} is the Kronecker delta and $\delta(\omega - \omega')$ is the delta function.

The interaction between the system and the reservoirs is described, in the rotating wave approximation (RWA), by

$$H_{SR} = \hbar \sqrt{\frac{\gamma'_m}{\pi}} \int d\omega e^{i\phi_m} a^\dagger c_m(\omega) + \text{h.c.} + \hbar \sqrt{\frac{\gamma'_1}{2\pi}} \int d\omega e^{i\phi_{q1}} \sigma_+ c_{q1}(\omega) + \text{h.c.} + \hbar \sqrt{\frac{\gamma'_\varphi}{4\pi}} \int d\omega e^{i\phi_{q\varphi}} \sigma_z c_{q\varphi}(\omega) + \text{h.c.}, \quad (11)$$

where we have used the raising and lowering operators

$$\sigma_+ = \frac{1}{2}(\sigma_x + i\sigma_y) \\ \sigma_- = \frac{1}{2}(\sigma_x - i\sigma_y). \quad (12)$$

Note that the coupling between the reservoir and system operators is assumed to be sufficiently broad-banded and slowly varying, on the scale of characteristic frequencies of the system, to be approximated as constant. We have also neglected the radiative correction of the oscillation frequencies. In addition, we have assumed that the spin-flip transitions occur between the two eigenstates of σ_z —this approximation is valid as long as $\hbar \Delta \ll \varepsilon_0$, which is the usual case with flux qubits (see, for example, Refs. 28 and 31).

2. Bloch-Langevin equations

Solving for the time evolution of the reservoir operators in the Heisenberg picture and substituting the result into the equations of motion of the system operators, leads to the so-called quantum Langevin equation for the oscillator and the Bloch-Langevin equations for the qubit. If we define envelope operators such that

$$\begin{aligned}\sigma_-(t) &= \tilde{\sigma}_-(t)e^{-i\eta(t)}, \\ a(t) &= \tilde{a}(t)e^{-i\omega_m t},\end{aligned}\quad (13)$$

where

$$\eta(t) = \varepsilon_0 \left(\phi_{e0} t + \frac{\phi_{e1}}{\omega_d} \sin \omega_d t \right), \quad (14)$$

we obtain:

$$\begin{aligned}\dot{\tilde{\sigma}}_-(t) &= -ik(a(t) + a^\dagger(t))\sigma_-(t) - \left(\frac{\gamma'_1}{2} + \gamma'_\varphi\right)\tilde{\sigma}_-(t) \\ &\quad + i\frac{1}{2}\Delta e^{i\eta(t)}\sigma_z(t) + i\frac{1}{2}\mathcal{V}_{q1}(t)\sigma_z(t) \\ &\quad - i(\sigma_+(t)\mathcal{V}_{q\varphi}(t) + \mathcal{V}_{q\varphi}^\dagger(t)\sigma_-(t)),\end{aligned}\quad (15a)$$

$$\begin{aligned}\dot{\tilde{\sigma}}_z(t) &= i\Delta(\tilde{\sigma}_-(t)e^{-i\eta(t)} - \tilde{\sigma}_+(t)e^{i\eta(t)}) - \gamma'_1(1 + \sigma_z(t)) \\ &\quad + 2i(\mathcal{V}_{q1}^\dagger(t)\tilde{\sigma}_-(t) - \tilde{\sigma}_+(t)\mathcal{V}_{q1}(t)),\end{aligned}\quad (15b)$$

$$\dot{\tilde{a}}(t) = -\frac{\gamma'_m}{2}\tilde{a}(t) - i\frac{1}{2}k\sigma_z(t)e^{i\omega_m t} + \mathcal{V}_m(t), \quad (15c)$$

where

$$\begin{aligned}\mathcal{V}_{q1}(t) &= \sqrt{\frac{\gamma'_1}{2\pi}}e^{i\phi_{q1}} \int d\omega e^{-i\omega(t-t_0)} c_{q1}(t_0, \omega), \\ \mathcal{V}_{q\varphi}(t) &= \sqrt{\frac{\gamma'_\varphi}{4\pi}}e^{i\phi_{q\varphi}} \int d\omega e^{-i\omega(t-t_0)} c_{q\varphi}(t_0, \omega), \\ \mathcal{V}_m(t) &= -i\sqrt{\frac{\gamma'_m}{\pi}}e^{i\phi_m} \int d\omega e^{-i\omega(t-t_0)} c_m(t_0, \omega).\end{aligned}\quad (16)$$

The derivation of these equations is standard, and can be found, e.g., in complements C_{IV} and A_V of Ref. 33. We now average (15) over the degrees of freedom of the reservoirs, which we assume are in thermal equilibrium with temperature T . Let us denote

$$\sigma_z^R = \text{Tr}_R[\rho_R \sigma_z],$$

where

$$\rho_R = \frac{\exp\left(-\frac{H_R}{k_B T}\right)}{\text{Tr}_R\left[\exp\left(-\frac{H_R}{k_B T}\right)\right]} \quad (17)$$

is the density operator of the reservoir and k_B is Boltzmann's constant, and Tr_R is the partial trace over the reservoir coordinates. With a similar definition for the

other system operators, we obtain the following equations:

$$\begin{aligned}\dot{\tilde{\sigma}}_-^R(t) &= -\gamma_2 \tilde{\sigma}_-^R(t) + i\frac{1}{2}\Delta \sigma_z^R(t)e^{i\eta(t)} \\ &\quad - ik(a^R(t) + a^{\dagger R}(t))\tilde{\sigma}_-^R(t),\end{aligned}\quad (18a)$$

$$\begin{aligned}\dot{\tilde{\sigma}}_z^R(t) &= -\gamma_1(\sigma_z^R(t) - \sigma_{z,\text{eq}}) \\ &\quad + i\Delta(\tilde{\sigma}_-^R(t)e^{-i\eta(t)} + \tilde{\sigma}_+^R(t)e^{i\eta(t)}),\end{aligned}\quad (18b)$$

$$\dot{\tilde{a}}^R(t) = -\frac{\gamma_m}{2}\tilde{a}^R(t) - i\frac{1}{2}k\sigma_z^R(t)e^{i\omega_m t}, \quad (18c)$$

where

$$\begin{aligned}\gamma_1 &= \frac{1}{2}\gamma'_1(2\hat{n}_0 + 1), \\ \gamma_\varphi &= \gamma'_\varphi(2\hat{n}_0 + 1), \\ \gamma_2 &= \gamma_1 + \gamma_\varphi, \\ \sigma_{z,\text{eq}} &= -\tanh \frac{\varepsilon_0 \phi_{e0}}{2k_B T},\end{aligned}\quad (19)$$

with

$$\hat{n}_0 = \left(\exp\left(\frac{\varepsilon_0 \phi_{e0}}{k_B T}\right) - 1 \right)^{-1}$$

the mean occupation number of the qubit reservoirs.

D. Passage to rotating frame

We may eliminate the explicit time dependence in (18) by performing the RWA as described in appendix C of Ref. 34. In most experimental setups, ε_0 is significantly larger than $\hbar\omega_d$, and the flux driving of the qubit may be very strong, with^{31,35} $\varepsilon_0 \phi_{e1} > \hbar\omega_d \gg \hbar\Delta$. We therefore need to consider the possibility of multi-photon Rabi oscillations, whereby $\varepsilon_0 \phi_{e0} \simeq n\hbar\omega_d$ for a particular integer n , and all other harmonics of ω_d are far from $\varepsilon_0 \phi_{e1}/\hbar$. In this case we may define

$$\delta = \frac{\varepsilon_0 \phi_{e0}}{\hbar} - n\omega_d. \quad (20)$$

Expansion of $e^{i\eta(t)}$ as a Fourier series then gives, under the RWA,

$$e^{i\eta(t)} = \sum_{l=-\infty}^{\infty} J_l\left(\frac{\varepsilon_0 \phi_{e1}}{\hbar\omega_d}\right) e^{i(\varepsilon_0 \phi_{e0}/\hbar - l\omega_d)t} \quad (21)$$

where J_n is a Bessel function of the first kind. Since all terms in (21) with $l \neq n$ will contribute rapidly rotating terms to the equations of motion (18), we can perform a RWA and neglect them, effectively substituting the factor $e^{i\eta(t)}$ by

$$J_n\left(\frac{\varepsilon_0 \phi_{e1}}{\hbar\omega_d}\right) e^{i\delta t}.$$

If we now return to the operators in the non-rotating frame, we eliminate the explicit time dependence, with the cost that now the analysis is confined to a multi-photon resonance with a particular n . Note that the additional modulation of the energy levels of the qubit due to the motion of oscillator is negligible in comparison to $\varepsilon_0\phi_{e1}$, and has therefore been ignored here.

E. Semiclassical approximation

Equations (18) together with the RWA made in the previous section, provide a complete specification of the properties of the system, under the assumptions made above. If, however, we are only interested in the stability properties of the system and in the possibility of existence of self-excited oscillations, it is sufficient to consider the semiclassical equation formed by averaging these equations over the degrees of freedom of the qubit and the oscillator. Furthermore, we note that when $k = 0$, the evolution of the qubit and the oscillator is independent. This implies that the covariance function between the oscillator and the qubit coordinates is of order k , which allows us to neglect them in the semiclassical equations when k is small. Under this assumption, all correlations of the system operators factorize, and we arrive at the following equations:

$$\dot{s}_-(t) = -\gamma_2 s_-(t) - i\delta s_-(t) + i\frac{1}{2}\Delta_n s_z(t) \quad (22a)$$

$$-ik(\alpha(t) + \alpha^*(t))s_-(t),$$

$$\dot{s}_z(t) = -\gamma_1(s_z(t) - \sigma_{z,\text{eq}}) + i\Delta_n(s_-(t) - s_+(t)), \quad (22b)$$

$$\dot{\alpha}(t) = -i\omega_m\alpha(t) - \frac{\gamma_m}{2}\alpha(t) - i\frac{1}{2}ks_z(t), \quad (22c)$$

where

$$\Delta_n = \Delta J_n \left(\frac{\varepsilon_0\phi_{e1}}{\hbar\omega_d} \right) \quad (23)$$

$$s_{\pm} = \langle \sigma_{\pm}^R \rangle_S, \quad s_z = \langle \sigma_z^R \rangle_S, \quad \alpha = \langle a^R \rangle_S, \quad (24)$$

and for an operator X ,

$$\langle X \rangle_S \equiv \text{Tr}_S[\rho X]. \quad (25)$$

Note that we have assumed that the degrees of freedom of the reservoir and of the system are statistically independent, and have made the so-called Born approximation for the reservoir.

These equations can also be written in vector form as

$$\dot{\mathbf{S}}(t) = M\mathbf{S}(t) + k\mathbf{g}(\mathbf{S}(t)) + \mathbf{S}_{\text{eq}}, \quad (26)$$

where M is a 5×5 matrix that represents the linear part of (22) that does not include the interaction term, $k\mathbf{g}(\mathbf{S}(t))$ is the interaction term and \mathbf{S}_{eq} is the inhomogeneous part of the system. The boldface coordinates represent a 5×1 vector, with

$$\mathbf{S}(t) = (s_-(t), s_+(t), s_z(t), \alpha(t), \alpha^*(t))^T. \quad (27)$$

III. ANALYSIS OF DYNAMICAL SYSTEM

In the case where the system is blue detuned, with $\delta = \varepsilon_0\phi_{e0}/\hbar - n\omega_d < 0$, the excess energy of the external flux driving is transferred to the mechanical oscillator^{18,20,32}, and is manifested in the system by a reduction of mechanical dissipation. As we will show, when the coupling exceeds a threshold, which we denote as k_c , the mechanical dissipation coefficient becomes negative, and the system loses its stability. This loss of stability, however, is of the “soft” type: self-excited oscillations emerge, with amplitudes that scale as $\sqrt{k - k_c}$, where k_c is the critical coupling. These oscillations are of the combined qubit-oscillator system, and their time dependence can be characterized by a single phase variable. In addition, since the beam is the element that loses stability, its dynamics enslaves those of the qubit, and the frequency of oscillations is equal to its renormalized frequency. In the terminology of nonlinear dynamics, the system is said to undergo a supercritical Hopf bifurcation. The quantitative details of this picture are provided in section (III C).

A. Centered equations of motion

The set of equations (22) is inhomogeneous, with a constant term in the right hand side. To proceed with the analysis, we first transform the coordinates to a set centered around an equilibrium point \mathbf{S}_{EP} . This equilibrium point is obtained by expansion in powers of k , namely

$$\mathbf{S}_{\text{EP}} = \mathbf{S}_{\text{EP},0} + k\mathbf{S}_{\text{EP},1} + k^2\mathbf{S}_{\text{EP},2} + \dots, \quad (28)$$

where $\mathbf{S}_{\text{EP},0}$ is the single solution of the system when $k = 0$. We find the following set of equations:

$$\begin{aligned} \dot{s}_{c-}(t) &= -\gamma_2 s_{c-}(t) - i\left(\tilde{\delta} + k(\alpha_c(t) + \alpha_c^*(t))\right)s_{c-}(t) \\ &\quad + \frac{1}{2}i\Delta_n s_{cz}(t) - ik_s(\alpha_c(t) + \alpha_c^*(t)) \end{aligned} \quad (29a)$$

$$\dot{s}_{cz}(t) = -\gamma_1 s_{cz}(t) + i\Delta_n(s_{c-}(t) - s_{c+}(t)) \quad (29b)$$

$$\dot{\alpha}_c(t) = -\frac{1}{2}\gamma_m\alpha_c(t) - i\omega_m\alpha_c(t) - \frac{1}{2}iks_{cz}(t), \quad (29c)$$

where $\mathbf{S}_c(t) = \mathbf{S}(t) - \mathbf{S}_{\text{EP}}$, and

$$\begin{aligned} \tilde{\delta} &= \delta - \frac{\delta^2\zeta_{\text{eq}}k^2}{\omega_m}, \\ k_s &= \frac{1}{2}\zeta_{\text{eq}}k\Delta_n(\delta + i\gamma_2), \\ \zeta_{\text{eq}} &= \frac{\gamma_1\sigma_{z,\text{eq}}}{\delta^2\gamma_1 + \Delta_n^2\gamma_2}. \end{aligned} \quad (30)$$

We have also assumed that both the dissipation and the coupling are small, namely that $\gamma_1 \simeq \gamma_2 \ll \delta \simeq \Delta_n$, $\gamma_m \ll \omega_m$, and $k \ll \omega_m$, and that ω_m is never significantly larger than

$$\Omega_R = \sqrt{\delta^2 + \Delta_n^2},$$

the Rabi frequency of the qubit. The salient feature of (29) is that now we see that the oscillator interacts with the qubit through a linear driving term in (29a), in addition to the nonlinear frequency-shifting term found in (22a).

B. Stability and renormalized mechanical eigenvalue

Since the stability of any dissipative dynamical system is determined solely by its linear part, we characterize the stability of (29) by neglecting its nonlinearity, and find an expression for the renormalized mechanical eigenvalues, which we denote as $\lambda_{\pm} = -\frac{1}{2}\tilde{\gamma}_m \pm i\tilde{\omega}_m$. Linearization gives us an approximate equation of the form $\dot{\mathbf{S}}_c = \mathcal{J}\mathbf{S}_c$, where

$$\mathcal{J} = \begin{pmatrix} -\gamma_2 - i\tilde{\delta} & 0 & \frac{1}{2}i\Delta_n & -ik_s & -ik_s \\ 0 & -\gamma_2 + i\tilde{\delta} & -\frac{1}{2}i\Delta_n & ik_s^* & ik_s^* \\ i\Delta_n & -\Delta_n & -\gamma_1 & 0 & 0 \\ 0 & 0 & -\frac{1}{2}ik & -\frac{1}{2}\gamma_m - i\omega_m & 0 \\ 0 & 0 & \frac{1}{2}ik & 0 & -\frac{1}{2}\gamma_m + i\omega_m \end{pmatrix} \quad (31)$$

is the Jacobian of the system. We are now facing the problem of finding the eigenvalues of \mathcal{J} . This can be achieved using perturbation theory, as shown in appendix A. We will follow, however, a different approach that yields identical results, yet has the benefit of providing considerable physical insight and can be applied to general problems that involve linearly interacting subsystems.

We will focus our attention on the qubit and on the oscillator separately, regarding both of them as input-output systems. From the form of linear part of (29), we can see that it is possible to regard $\alpha_c(t) + \alpha_c^*(t)$ as the input of the qubit, and $s_{cz}(t)$ as the input of the oscillator. If we also regard $s_{cz}(t)$ as the output of the qubit and $\alpha_c(t) + \alpha_c^*(t)$ as the output of the oscillator, we can decompose the matrix into two separate 3×3 and 2×2 blocks. This simplifies the analysis considerably, and provides physical insight into the behavior of the qubit under linear driving of the type seen in (29a). As we will see, the stability of the system and the renormalized mechanical eigenvalues λ_{\pm} are determined mostly by the response of the qubit to the linear driving term in (29a)—in particular, we will show in subsection III B 2 that

$$\begin{aligned} \tilde{\gamma}_m &= \gamma_m - k \operatorname{Im} \chi_z, \\ \tilde{\omega}_m &= \omega_m + \frac{1}{2}k \operatorname{Re} \chi_z, \end{aligned} \quad (32)$$

where χ_z is the qubit response function. We therefore begin by deriving an approximate expression for χ_z and discussing its properties.

1. Qubit response function

To derive χ_z , the response function of the qubit, we assume that the time dependence of the oscillator is a general complex sinusoid of the form $\alpha_c(t) = \alpha_0 e^{st}$, where

s is complex. Due to the linearity of the system, the steady state response of the z component of the qubit, $s_{cz}(t)$, will be given by $\chi_z(s)\alpha_0 e^{st}$. This function, as well as the response functions of $s_{c-}(t)$ and $s_{c+}(t)$, are given by

$$\begin{pmatrix} \chi_- \\ \chi_+ \\ \chi_z \end{pmatrix} = -(\mathcal{J}^{(3)} - sI_3)^{-1} \begin{pmatrix} -ik_s \\ ik_s^* \\ 0 \end{pmatrix}, \quad (33)$$

where $\mathcal{J}^{(3)}$ is the upper left 3×3 block of \mathcal{J} , and I_3 is the 3×3 identity matrix. Invoking the assumptions on the values of the parameters made in section III A and using $\gamma_{\varphi} = \gamma_2 - \gamma_1$, we have

$$\chi_z(s) \simeq \frac{\delta\zeta_{\text{eq}} k \Delta_n^2 (s + 2\gamma_2)}{(s + \tilde{\gamma}_1)(s + \tilde{\gamma}_2 + i\bar{\Omega}_R)(s + \tilde{\gamma}_2 - i\bar{\Omega}_R)}, \quad (34)$$

where

$$\begin{aligned} \tilde{\gamma}_1 &= \gamma_1 + \frac{\Delta_n^2}{\Omega_R^2} \gamma_{\varphi}, \\ \tilde{\gamma}_2 &= \gamma_2 - \frac{\Delta_n^2}{2\Omega_R^2} \gamma_{\varphi}, \\ \bar{\Omega}_R &= \Omega_R - \frac{4\gamma_2^2 \Omega_R^4 + \gamma_{\varphi}^2 \Delta_n^2 (4\delta^2 + \Delta_n^2)}{\Omega_R^5}. \end{aligned} \quad (35)$$

The location of the poles and zeros of (34) is correct to second order in the small parameters. A plot of the real and imaginary parts of $\chi_z(-i\omega)$ can be found in Fig. 3, and a plot of χ_z as a function of ω and δ is given in Fig. 2. Note that the correction for the Rabi frequency, $\bar{\Omega}_R - \Omega_R$, is of second order in the small parameters, and thus can be neglected in what follows. Note that $\tilde{\gamma}_1$ and $\tilde{\gamma}_2$ correspond to the approximate decay constants in the diagonal coordinate system of the qubit, provided that γ_1 and γ_2 are small compared to Ω_R . This will be shown explicitly in appendix B, where the diagonal coordinates of the qubit will be found.

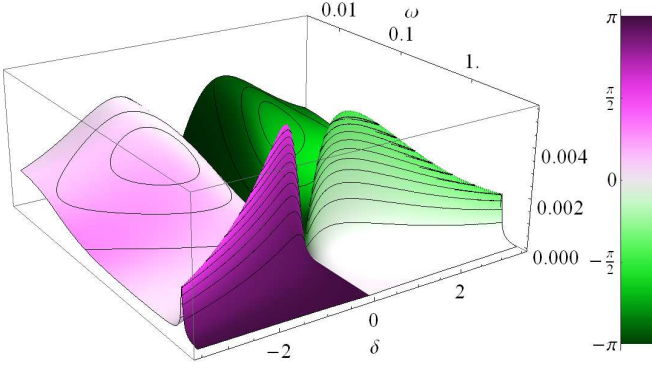


FIG. 2. (Color online) The response function $\chi_z(-i\omega)$ as given in (34), as a function of δ and ω . The vertical axis corresponds to the absolute value, the color corresponds to the phase, and the contours correspond to the imaginary part. For all $\delta < 0$, the phase is positive, which implies that the qubit adds delay, thus decreasing the effective dissipation constant of the oscillator. (Recall that we are considering negative frequencies.) For $\delta > 0$, the opposite is true. Parameters are given in Table I.

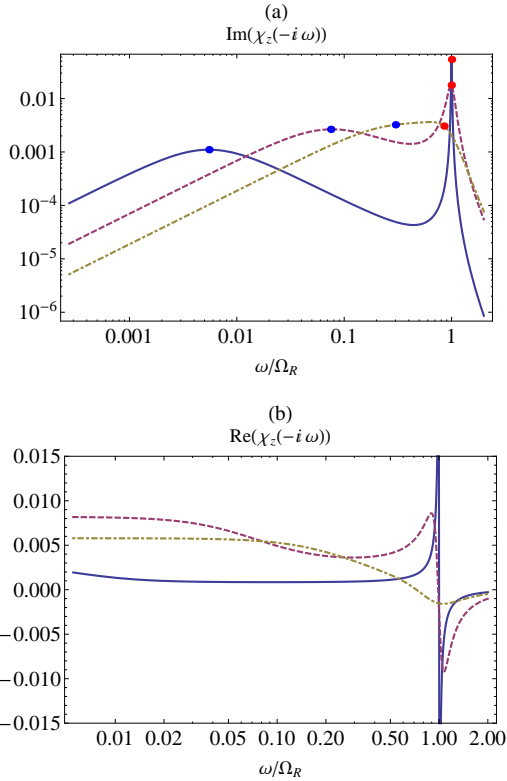


FIG. 3. (Color online) The imaginary (a) and real (b) parts of the qubit response function, $\chi_z(-i\omega)$, as given by (34) in the blue-detuned ($\delta < 0$) regime, for different qubit decay times γ_1 and γ_2 . The blue dots in (a) corresponds to the maximum at $\omega = \tilde{\gamma}_1$, and the red dots to the maximum at $\omega = \bar{\Omega}_R$. Solid line: $\gamma_1 = 0.001$, $\gamma_2 = 0.01$. Dashed line: $\gamma_1 = 0.05$, $\gamma_2 = 0.1$. Dot-dashed line: $\gamma_1 = 0.1$, $\gamma_2 = 0.5$. Other parameters are given in Table I.

2. Renormalization of mechanical eigenvalue

To derive (32), let us consider the qubit as a part of the full system. Since the Q -factor of the mechanical oscillator, $Q = \frac{\omega_m}{\gamma_m}$, is typically high (of the order $\sim 10^5$), we can expect that any excitation at a frequency far from ω_m will not be sustained by the system, and that the decay or growth times of the oscillator are very long. This allows us to assume that the qubit is driven by a signal of the form $\alpha_0 e^{-i\omega_m t} + \text{c.c.}$, and due to linearity, the z -component of the Bloch vector of the qubit responds as $s_{cz}(t) = \chi_z(-i\omega_m)\alpha_0 e^{-i\omega_m t} + \text{c.c.}$ Substituting this response in the equation for α_c in (29c) and keeping only resonant terms, we find that under this approximation we have

$$\dot{\alpha}_c(t) = -\frac{1}{2}\tilde{\gamma}_m\alpha_c(t) - i\tilde{\omega}_m\alpha_c(t), \quad (36)$$

where $\tilde{\gamma}_m$ and $\tilde{\omega}_m$ are given by (32).

3. Nearly adiabatic case

In this case we assume that $\omega_m \ll \Omega_R$, and that $\omega_m \simeq \gamma_1, \gamma_2$, so that ω_m is also a small parameter. Substituting $s = -i\omega_m$ in (34) and keeping only small terms only up to second order, we find that

$$\chi_z(-i\omega_m) \simeq \frac{\delta\zeta_{\text{eq}}k\Delta_n^2(\omega_m + 2i\gamma_2)}{\Omega_R^2(\omega_m + i\tilde{\gamma}_1)}. \quad (37)$$

Substituting this into (32), we find that

$$\tilde{\gamma}_m = \gamma_m - \frac{\delta\zeta_{\text{eq}}k^2\Delta_n^2(\gamma_2\Omega_R^2 + \delta^2\gamma_\varphi)}{\Omega_R^4} \frac{\omega_m}{\tilde{\gamma}_1^2 + \omega_m^2}, \quad (38)$$

and

$$\tilde{\omega}_m = \omega_m + \frac{\delta\zeta_{\text{eq}}k^2\Delta_n^2}{2\Omega_R^2} \frac{2\gamma_2\tilde{\gamma}_1 + \omega_m^2}{\tilde{\gamma}_1^2 + \omega_m^2}. \quad (39)$$

Note that because $\gamma_\varphi > 0$, the sign of the correction to γ_m in (38) depends only on the sign of δ , and is negative for blue detuning and positive for red detuning, as expected.

As we can see, the critical coupling k_c , that can be found by equating (38) to zero, depends strongly on the relation between the characteristic time scales of the qubit and the oscillator, and in particular on the ratio ω_m/Ω_R . The interaction is maximal at the resonance, $\omega_m/\Omega_R \simeq 1$, and exhibits another smaller peak at $\omega_m = \tilde{\gamma}_1$, where $\tilde{\gamma}_1$ is defined in (35). Outside the range $\tilde{\gamma}_1 < \omega_m < \Omega_R$, the interaction is weak. This dependence is illustrated in Fig. 3 which plots (34). From a control systems point of view, we can see that the qubit approximately responds as a harmonic oscillator with natural frequency Ω_R and decay constant γ_m , connected in series to a lag compensator with a much slower time scale. This implies that when $\delta < 0$, the qubit will reduce the effective dissipation coefficient for any set of values of the other parameters, and when $\delta > 0$, the opposite is true.

4. Resonance case

When $\omega_m \simeq \Omega_R$, the qubit and the oscillator are resonant, and the interaction is maximal. In this case, the correction of the mechanical dissipation coefficient, $\tilde{\gamma}_m - \gamma_m$, becomes of first order in the small parameters of the system, and in fact overwhelms γ_m for high quality oscillators. To derive an expression for χ_z near resonance, we set

$$\omega_m = \Omega_R + \sigma, \quad (40)$$

where σ is a small parameter. We then get

$$\chi_z(-i(\Omega_R + \sigma)) \simeq -\frac{\delta\zeta_{\text{eq}}k\Delta_n^2}{2\Omega_R(\sigma + i\tilde{\gamma}_2)}, \quad (41)$$

which gives

$$\tilde{\gamma}_m = \gamma_m - \frac{\delta\zeta_{\text{eq}}k^2\tilde{\gamma}_2\Delta_n^2}{2\Omega_R(\tilde{\gamma}_2^2 + \sigma^2)} \quad (42)$$

and

$$\tilde{\omega}_m = \omega_m - \frac{\delta\zeta_{\text{eq}}k^2\Delta_n^2\sigma}{4\Omega_R(\tilde{\gamma}_2^2 + \sigma^2)}. \quad (43)$$

The general behavior of the correction to the mechanical dissipation coefficient, as a function of the DC and AC parts of the external applied flux, $\varepsilon_0\phi_{e0}$ and $\varepsilon_0\phi_{e1}$, can be seen in Fig. 4. This result was obtained by superposing the corrections for different values of n , the multi-photon Rabi resonance, as defined in (20). This result may be compared to the Landau-Zener interference diagrams, given in Refs. 31 and 34.

C. Hopf bifurcation at resonance regime

In this section, we no longer neglect the nonlinear part of (29). We also continue assuming that $\delta < 0$ so that the system is blue-detuned. We will derive approximate analytical expressions for the limit cycle amplitude and frequency, under the assumption that the system is approximately resonant, i.e. that $\omega_m \simeq \Omega_R$, using the method of averaging (chapter 11 of Ref. 36). This is accomplished by first diagonalizing M_0 , the large part of M in (26) defined in (B1), and then transforming to a frame rotating at ω_m . This will essentially give us an equation for the envelopes of components of the qubit on the Bloch sphere and of the amplitude of the oscillator, which are slowly varying. The equilibrium points of this set of equations, then, will give the amplitude of the limit cycle, while the equation for the phase of these envelopes will provide the frequency of oscillations.

1. Approximated equations of motion

The set of equations described above is given by

$$\dot{\bar{s}}_{c-}(t) = -(\tilde{\gamma}_2 - i\sigma)\bar{s}_{c-}(t) \quad (44a)$$

$$-ik\bar{\Delta}_n\bar{a}_c(t)(\bar{s}_{cz}(t) + s_{z,\text{eq}}),$$

$$\dot{\bar{s}}_{cz}(t) = -\tilde{\gamma}_1\bar{s}_{cz}(t) \quad (44b)$$

$$-2ik\bar{\Delta}_n(\bar{a}_c^*(t)\bar{s}_{c-}(t) - \bar{s}_{c+}(t)\bar{a}_c(t)),$$

$$\dot{\bar{a}}_c(t) = -\frac{1}{2}\gamma_m\bar{a}_c(t) + ik\bar{\Delta}_n\bar{s}_{c-}(t), \quad (44c)$$

where

$$\bar{\Delta}_n = \frac{\Delta_n}{2\Omega_R},$$

σ is the small detuning from resonance, defined in (40), and $s_{z,\text{eq}} = \delta\Omega_R\zeta_{\text{eq}}$. These equations are derived in appendix B, using the procedure outlined above. Note that $s_{z,\text{eq}} > 0$ for blue detuning—this corresponds to an effective inversion of the energy levels of the qubit.

Since these are envelope equations, we can obtain a detailed picture of the behavior of the system near resonance by finding their equilibrium points. Specifically, we will show that for $\tilde{\gamma}_m > 0$, where $\tilde{\gamma}_m$ is as defined in (42), the system will have a single stable equilibrium at the origin, while for $\tilde{\gamma}_m < 0$, the origin will lose its stability and a new set of equilibrium points will emerge. In the approximated system (44), this change is a supercritical pitchfork bifurcation, while for the original equations in (29), it corresponds to a supercritical Hopf bifurcation.

2. Limit cycle solution

To find the non-trivial equilibrium points of (44), we begin by assuming that during the limit cycle, the phase difference between \bar{a}_c and \bar{s}_{cz} remains constant, which is required by the periodicity of the limit cycle. Therefore, we can set:

$$\bar{a}_c = r_a \exp(i\omega_a t) \quad (45)$$

$$\bar{s}_{c-} = r_s \exp\left[i\left(\omega_a t - \frac{\pi}{2} + f(\sigma)\right)\right],$$

where r_s , r_a , ω_a and $f(\sigma)$ are real, and the form for the phase of \bar{s}_{c-} was chosen so that $f(\sigma) = 0$ for $\sigma = 0$. When the system is in a limit cycle state, both the radii r_s and r_a and \bar{s}_{cz} are constant in time, and we have assumed that ω_a is constant as well. Therefore, substitution of these definitions into (44) gives a set of equations for the equilibrium point that can be solved exactly. This set has a nontrivial solution only for $k > k_c$, where

$$k_c = \sqrt{\frac{2\gamma_m\Omega_R(\tilde{\gamma}_2^2 + \sigma^2)}{\delta\zeta_{\text{eq}}\tilde{\gamma}_2\Delta_n^2}}, \quad (46)$$

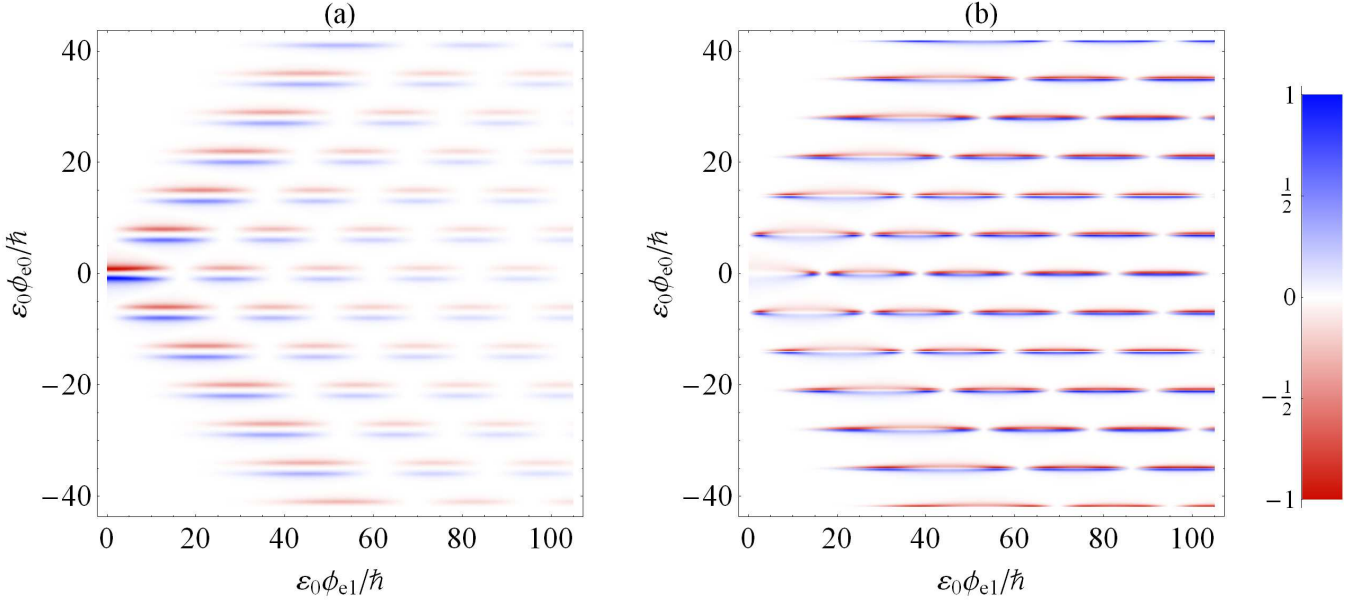


FIG. 4. (Color online) Correction of dissipation coefficient as a function of external flux driving amplitude, $\varepsilon_0\phi_{e1}/\hbar$, and detuning, $\varepsilon_0\phi_{e0}/\hbar$. The blue areas corresponds to a decrease, and the red to an increase, in the effective mechanical dissipation coefficient. The color intensities are scaled by the extremal values of the correction. Panel (a) corresponds to the resonance regime, with $\omega_m = 1.28\Delta$, and panel (b) corresponds to the nearly adiabatic regime, with $\omega_m = 0.14\Delta$. The values of the correction are given in arbitrary units. Parameters used are: $\gamma_1 = 0.014\omega_d$, $\gamma_2 = 0.714\omega_d$, $k = 0.0018\omega_d$, $\sigma_{z,\text{eq}} = -1$, $\Delta = 0.1\omega_d$, and $Q = 10^5$. This plot may be compared to Refs. 31 and 34.

and we have neglected γ_m in comparison with $\bar{\gamma}_2$. Note that this is the same critical coupling as that given by (42). (The assumption that $\bar{\gamma}_2 \gg \gamma_m$ was made in section III B when we assumed that the input to the qubit is a non-damped sinusoid.) The nontrivial solution is given by:

$$\begin{aligned}
 r_s &= \frac{s_{z,\text{eq}}}{2} \sqrt{\frac{\bar{\gamma}_1}{\bar{\gamma}_2}} \frac{k_c^2}{k^2} \sqrt{\frac{k^2}{k_c^2} - 1}, \\
 r_a &= \sqrt{\frac{\bar{\gamma}_1 s_{z,\text{eq}}}{2\gamma_m}} \frac{k_c}{|k|} \sqrt{\frac{k^2}{k_c^2} - 1}, \\
 s_{cz} &= s_{z,\text{eq}} \left(\frac{k_c^2}{k^2} - 1 \right), \\
 \omega_a &= \frac{\gamma_m \sigma}{2\bar{\gamma}_2 + \gamma_m}, \\
 f(\sigma) &= \arctan \frac{2\sigma}{2\bar{\gamma}_2 + \gamma_m}.
 \end{aligned} \tag{47}$$

This solution provides a complete characterization of the limit cycle near resonance. We can see that the system has a limit cycle for $k > k_c$, with amplitudes proportional to $\sqrt{k - k_c}$, as is the case with non-degenerate supercritical Hopf bifurcations. Furthermore, the frequency of the limit cycle solution undergoes a shift proportional to σ , as can be seen in the equation for ω_a in (47). In Fig. 5 we can see the bifurcation curves for the system near resonance, which were calculated using numerical continuation³⁷.

In the nearly adiabatic regime the interaction is of second order in k . It turns out that bifurcation analysis of the approximated equations of the form (44) for this regime is analytically intractable. Numerical analysis, however, indicates that the Hopf bifurcation in this regime is supercritical as well, with behavior similar to that seen in the resonance regime.

IV. DISCUSSION AND CONCLUSIONS

We have characterized the stability properties of a flux qubit coupled to a mechanical oscillator and its nonlinear behavior near resonance. We have found that the interaction between the qubit and the oscillator is typically non-

Parameter	Value
γ_1	$0.01\Omega_R$
γ_2	$0.1\Omega_R$
δ	$-0.707\Omega_R$
Δ	$0.707\Omega_R$
k	$0.013\Omega_R$
$\sigma_{z,\text{eq}}$	-1
Q	10^5

TABLE I. Numerical parameters used in the generation of Figures 3, 2 and 5

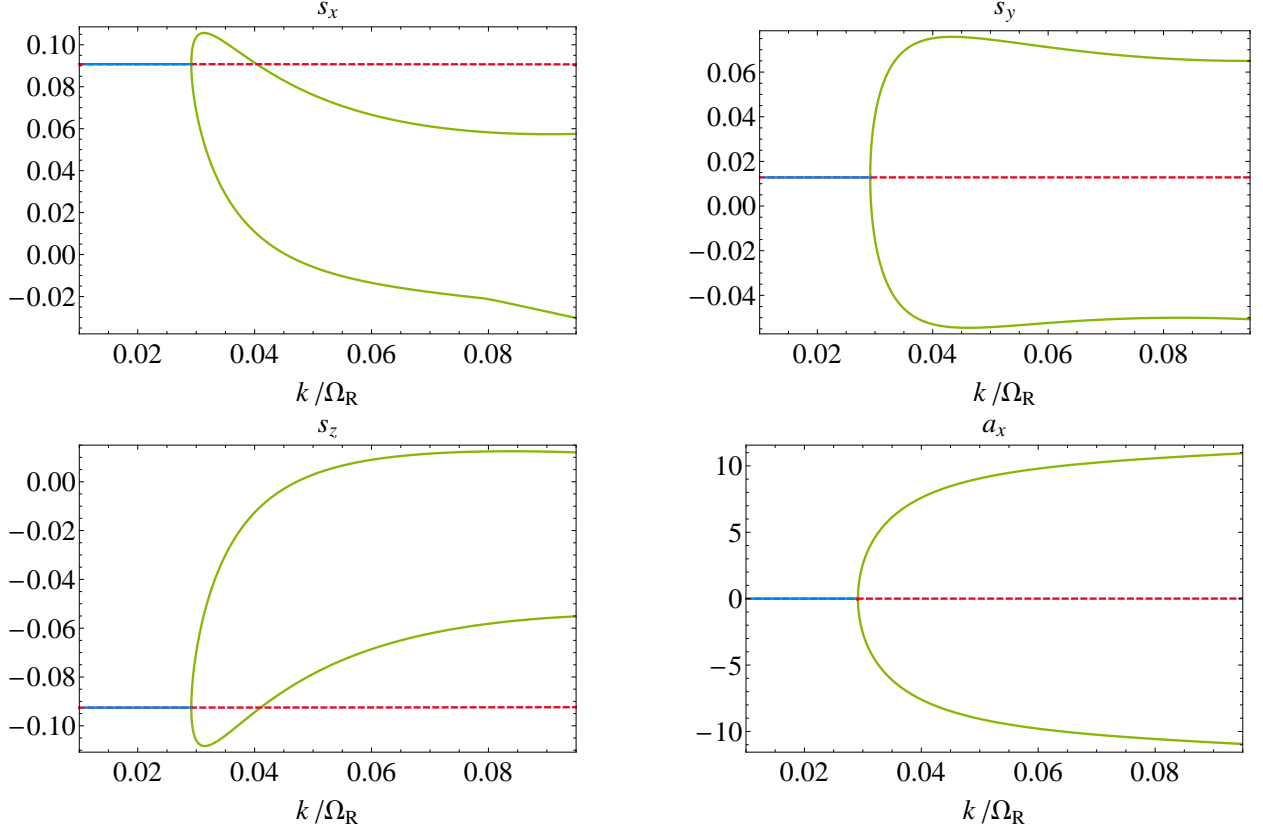


FIG. 5. (Color online) Bifurcation curves for the system near resonance, with $\omega_m = 1.1\Omega_R$. The blue and dashed red lines corresponds to stable and non-stable equilibrium points, respectively. The green curve corresponds to a stable limit cycle, where the top curves corresponds to the maximal value of the variable during the limit cycle, and the bottom curve corresponds to the minimal value. Numerical values used in the simulation are given in table I.

negligible only over a range of oscillator frequencies that begins with $\omega_m \simeq \bar{\gamma}_1$, which we denoted as the nearly-adiabatic regime, and ends with $\omega_m \simeq \Omega_R$, which we denoted as the resonance regime. The interaction near the resonance regime is significantly stronger. We have found that sign of the correction factor for the mechanical dissipation coefficient γ_m depends only on sign of the detuning parameter δ .

We have also found that near resonance, when the critical coupling is exceeded, the system undergoes a supercritical Hopf bifurcation. Numerical analysis indicates that the bifurcation at the nearly adiabatic regime is supercritical as well.

The method used in the stability analysis of this system, namely the decomposition into interacting subsystems, is general in nature and can be applied to any set of weakly interacting subsystems, yielding considerable physical insight into their behavior.

The limit cycle behavior of this system suggests a possible scheme for the preparation of non-classical entangled states of the qubit and oscillator: Since the limit cycle dynamics can be described by a single phase variable, if the system is cooled to its ground state so that thermal noise is negligible and then rapidly brought to a

limit cycle state, this phase variable can be expected to be found in a superposition state. A more quantitative analysis of this point is left to subsequent articles.

V. ACKNOWLEDGMENTS

The authors would like to thank Gil Bachar and Nahum Shimkin for their valuable input. This work was supported by the German Israel Foundation under Grant No. 1-2038.1114.07, the Israel Science Foundation under Grant No. 1380021 and the European STREP QNEMS Project.

Appendix A: Perturbation analysis of mechanical eigenvalue

The main results regarding the renormalized mechanical eigenvalues λ_{\pm} , (38), (39), (42) and (43), can also be obtained by using perturbation analysis for \mathcal{J} , under the assumption that k is a small parameter. Let us denote

$$\mathcal{J} = \mathcal{J}_0 + k\mathcal{J}_1, \quad (\text{A1})$$

where $k\mathcal{J}_1$ is the part of \mathcal{J} proportional to k . We also denote $\lambda_{0+} = -\frac{1}{2}\gamma_m + i\omega_m$ as the mechanical eigenvalue of \mathcal{J}_0 , and \mathbf{v}_m as its corresponding eigenvector. We now denote \mathcal{R} as the inverse of the upper 4×4 part of $\lambda_+ I_5 - \mathcal{J}_0$, namely the matrix satisfying

$$(\lambda_+ I_5 - \mathcal{J}_0) \mathcal{R} = \mathcal{R} (\lambda_+ I_5 - \mathcal{J}_0) = I_5 - \mathbf{v}_m \mathbf{v}_m^T, \quad (\text{A2})$$

where I_5 is the 5×5 identity matrix. It is then possible to show that λ_+ can be expanded in a power series in k , where

$$\lambda_+ = \lambda_{0+} + k \mathbf{v}_m^T \mathcal{J}_k \mathbf{v}_m + k^2 \mathbf{v}_m^T \mathcal{R} \mathcal{J}_k \mathcal{R} \mathbf{v}_m + O(k^3). \quad (\text{A3})$$

The term proportional to k is equal to zero, and the term proportional to k^2 gives the approximate results obtained above.

Appendix B: Approximated Equations for resonance regime

To derive the approximated equations for the envelopes (44), we begin by diagonalizing the large part of (26), as explained above. Let us define $M = M_0 + M_1$. In the basis defined by (27),

$$M_0 = i \left(\begin{array}{ccc|cc} -\delta & 0 & \frac{1}{2}\Delta_n & & \\ 0 & \delta & -\frac{1}{2}\Delta_n & & \\ -\Delta_n & \Delta_n & 0 & & \\ \hline & & 0 & -\omega_m & 0 \\ & & & 0 & \omega_m \end{array} \right) \quad (\text{B1})$$

is the large part of M , and therefore of (26), and M_1 contains the smaller dissipative terms on the diagonal. The diagonalizing matrix of the upper 3×3 block of this M_0 , which we denote as $M_0^{(3)}$, is given by

$$Q^{(3)} = \left(\begin{array}{cc|c} \frac{1}{2} \left(\frac{\delta}{\Omega_R} + 1 \right) & \frac{1}{2} \left(\frac{\delta}{\Omega_R} - 1 \right) & \frac{\Delta_n}{2\Omega_R} \\ \frac{1}{2} \left(\frac{\delta}{\Omega_R} - 1 \right) & \frac{1}{2} \left(\frac{\delta}{\Omega_R} + 1 \right) & \frac{\Delta_n}{2\Omega_R} \\ \hline -\frac{\Delta_n}{\Omega_R} & -\frac{\Delta_n}{\Omega_R} & \frac{\delta}{\Omega_R} \end{array} \right), \quad (\text{B2})$$

and

$$D^{(3)} = \left(Q^{(3)} \right)^{-1} M_0^{(3)} Q^{(3)} = \left(\begin{array}{ccc} -i\Omega_R & 0 & 0 \\ 0 & i\Omega_R & 0 \\ 0 & 0 & 0 \end{array} \right). \quad (\text{B3})$$

Next, we note that close to resonance, $\sigma = \omega_m - \Omega_R$ is a small parameter. Therefore,

$$D = \left(\begin{array}{c|cc} D^{(3)} & 0 & \\ \hline 0 & -i\omega_m & 0 \\ & 0 & i\omega_m \end{array} \right)$$

can be separated to a large part D_0 , proportional to ω_m , and to a small part D_σ , proportional to σ . We can now define a set of envelope coordinates $\bar{\mathbf{S}}_c(t)$ such that $\mathbf{S}_c(t) = Q e^{D_0 t} \bar{\mathbf{S}}_c(t)$. Explicitly:

$$\bar{\mathbf{S}}_c(t) = (\bar{s}_{c-}(t), \bar{s}_{c+}(t), \bar{s}_{cz}(t), \bar{\alpha}_c(t), \bar{\alpha}_c^*(t))^T, \quad (\text{B4})$$

and

$$Q = \left(\begin{array}{c|c} Q^{(3)} & 0 \\ \hline 0 & I_2 \end{array} \right)$$

where I_2 is the 2×2 identity matrix. When substituting (B4) into (26), we obtain the equation

$$\dot{\bar{\mathbf{S}}}_c(t) = e^{-D_0 t} Q^{-1} (D_\sigma + M_1) Q e^{D_0 t} \bar{\mathbf{S}}_c(t) + k e^{-D_0 t} Q^{-1} \mathbf{g} (Q e^{D_0 t} \bar{\mathbf{S}}_c(t)), \quad (\text{B5})$$

Since all terms on the right hand side of this equation are small and $e^{D_0 t}$ contains a single frequency, ω_m , we can now perform the averaging approximation. This is achieved by integrating (B5) over a single period and keeping $\bar{\mathbf{S}}_c(t)$ constant:

$$\begin{aligned} \dot{\bar{\mathbf{S}}}_c(t) &\simeq \\ &\frac{1}{2\pi\omega_m^{-1}} \int_0^{2\pi\omega_m^{-1}} e^{-D_0 t'} Q^{-1} (D_\sigma + M_1) Q e^{D_0 t'} \bar{\mathbf{S}}_c(t) dt' \\ &+ \frac{k}{2\pi\omega_m^{-1}} \int_0^{2\pi\omega_m^{-1}} e^{-D_0 t'} Q^{-1} \mathbf{g} (Q e^{D_0 t'} \bar{\mathbf{S}}_c(t)) dt'. \end{aligned} \quad (\text{B6})$$

The integration will remove all terms in (B5) proportional to $e^{i\omega_m t}$ and its harmonics, and is in fact equivalent to performing an RWA. Equation (B6) is equal to the set (44).

* liore@tx.technion.ac.il

¹ S. Ashhab and F. Nori, Physical Review A **81**, 042311 (2010).

² E. Buks and M. P. Blencowe, Physical Review B **74**, 174504 (2006).

³ E. K. Irish, J. Gea-Banacloche, I. Martin, and K. C. Schwab, Physical Review B **72**, 195410 (2005).

⁴ S. Agarwal and J. H. Eberly, Physical Review A **86**, 022341 (2012).

⁵ J. Hauss, A. Fedorov, C. Hutter, A. Shnirman, and G. Schn, Physical Review Letters **100**, 037003 (2008).

⁶ M. Poot and H. S. van der Zant, Physics Reports **511**, 273 (2012).

⁷ J. Zhang, Y.-x. Liu, and F. Nori, Physical Review A **79**, 052102 (2009).

- ⁸ S. Etaki, M. Poot, I. Mahboob, K. Onomitsu, H. Yamaguchi, and H. S. J. van der Zant, *Nature Physics* **4**, 785 (2008).
- ⁹ S. Pugnetti, Y. M. Blanter, and R. Fazio, *EPL (Europhysics Letters)* **90**, 48007 (2010).
- ¹⁰ M. D. LaHaye, J. Suh, P. M. Echternach, K. C. Schwab, and M. L. Roukes, *Nature* **459**, 960 (2009).
- ¹¹ S. Pugnetti, Y. M. Blanter, F. Dolcini, and R. Fazio, *Physical Review B* **79**, 174516 (2009).
- ¹² M. Poot, S. Etaki, I. Mahboob, K. Onomitsu, H. Yamaguchi, Y. M. Blanter, and H. S. J. van der Zant, *Physical Review Letters* **105**, 207203 (2010).
- ¹³ P. Rabl, *Physical Review B* **82**, 165320 (2010).
- ¹⁴ F. Xue, Y. D. Wang, C. P. Sun, H. Okamoto, H. Yamaguchi, and K. Semba, *New Journal of Physics* **9**, 35 (2007).
- ¹⁵ M. Poot, S. Etaki, H. Yamaguchi, and H. S. J. van der Zant, *Applied Physics Letters* **99**, 013113 (2011).
- ¹⁶ Y.-D. Wang, Y. Li, F. Xue, C. Bruder, and K. Semba, *Physical Review B* **80**, 144508 (2009).
- ¹⁷ S. Etaki, M. Poot, K. Onomitsu, H. Yamaguchi, and H. S. van der Zant, *Comptes Rendus Physique* **12**, 817 (2011).
- ¹⁸ Y. S. Greenberg and E. Ilichev, *Physical Review B* **77**, 094513 (2008).
- ¹⁹ S. N. Shevchenko, A. N. Omelyanchouk, and E. Ilichev, *Low Temperature Physics* **38**, 283 (2012).
- ²⁰ M. Grajcar, S. H. W. v. d. Ploeg, A. Izmalkov, E. Ilichev, H.-G. Meyer, A. Fedorov, A. Shnirman, and G. Schn, *Nature Physics* **4**, 612 (2008).
- ²¹ S. D. Bennett and A. A. Clerk, *Physical Review B* **74**, 201301 (2006).
- ²² A. N. Omelyanchouk, S. N. Shevchenko, Y. S. Greenberg, O. Astafiev, and E. Ilichev, *Low Temperature Physics* **36**, 893 (2010).
- ²³ C. Vierheilg, J. Hausinger, and M. Grifoni, *Physical Review A* **80**, 052331 (2009).
- ²⁴ S. N. Shevchenko, S. H. W. van der Ploeg, M. Grajcar, E. Ilichev, A. N. Omelyanchouk, and H.-G. Meyer, *Physical Review B* **78**, 174527 (2008).
- ²⁵ I. Chiorescu, Y. Nakamura, C. J. P. M. Harmans, and J. E. Mooij, *Science* **299**, 1869 (2003).
- ²⁶ E. Ilichev, N. Oukhanski, A. Izmalkov, T. Wagner, M. Grajcar, H.-G. Meyer, A. Y. Smirnov, A. Maassen van den Brink, M. H. S. Amin, and A. M. Zagoskin, *Physical Review Letters* **91**, 097906 (2003).
- ²⁷ J. M. Martinis, S. Nam, J. Aumentado, and C. Urbina, *Physical Review Letters* **89**, 117901 (2002).
- ²⁸ J. E. Mooij, T. P. Orlando, L. Levitov, L. Tian, C. H. v. d. Wal, and S. Lloyd, *Science* **285**, 1036 (1999).
- ²⁹ T. P. Orlando, J. E. Mooij, L. Tian, C. H. van der Wal, L. S. Levitov, S. Lloyd, and J. J. Mazo, *Physical Review B* **60**, 15398 (1999).
- ³⁰ Y. Makhlin, G. Schn, and A. Shnirman, *Reviews of Modern Physics* **73**, 357 (2001).
- ³¹ D. M. Berns, W. D. Oliver, S. O. Valenzuela, A. V. Shytov, K. K. Berggren, L. S. Levitov, and T. P. Orlando, *Physical Review Letters* **97**, 150502 (2006).
- ³² M. Aspelmeyer, P. Meystre, and K. Schwab, *Physics Today* **65**, 29 (2012).
- ³³ C. Cohen-Tannoudji, J. Dupont-Roc, and G. Grynberg, *Atom - Photon Interactions: Basic Process and Applications* (Wiley, 2008).
- ³⁴ S. N. Shevchenko, S. Ashhab, and F. Nori, *Physics Reports* **492**, 1 (2010).
- ³⁵ A. Izmalkov, S. H. W. van der Ploeg, S. N. Shevchenko, M. Grajcar, E. Ilichev, U. Hbner, A. N. Omelyanchouk, and H.-G. Meyer, *Physical Review Letters* **101**, 017003 (2008).
- ³⁶ F. Verhulst, *Nonlinear Differential Equations and Dynamical Systems* (Springer, 1996).
- ³⁷ The program used was XPPAUT, see B. Ermentrout, *Simulating, Analyzing, and Animating Dynamical Systems: A Guide to Xppaut for Researchers and Students*, 1st ed. (Society for Industrial and Applied Mathematics, 2002).